Faculty of Science

Supraglacial lakes monitoring using SAR imagery at Jakobshavn Isbræ, Greenland

David Ek

Degree of Bachelor of Science
with a major in Earth Sciences
15 hec

Department of Earth Sciences
University of Gothenburg
2020 B-1090

UNIVERSITY OF GOTHENBURG

UNIVERSITY OF GOTHENBURG
Department of Earth Sciences
Geovetarcentrum/Earth Science Centre

Supraglacial lakes monitoring using SAR imagery at Jakobshavn Isbræ, Greenland

David Ek

ISSN 1400-3821

B1090
Bachelor of Science thesis
Göteborg 2020

Mailing address
Geovetarcentrum
S 405 30 Göteborg

Address
Geovetarcentrum
Guldhedsgatan 5A

Telephone
031-786 19 56

Geovetarcentrum
Göteborg University
S-405 30 Göteborg
SWEDEN

ABSTRACT

Supraglacial lakes are a common feature on the Greenland ice sheet. They are mainly found during the melt season which takes place during the summer months when there is a positive net energy flux between the atmosphere and the ice sheet surface which generates surface melt. The lakes can undergo rapid draining events through cracks and moulins causing large influxes of meltwater volumes to the ice-bedrock interface leading to enhanced basal sliding. As increased ice velocities are capable of transporting ice faster to the terminus, calving rates might increase, causing a direct impact on the mean sea level rise. The objective of this study is to monitor supraglacial lakes remotely using Sentinel-1 SAR imagery, and to assess the influence of supraglacial lake draining events on ice speed velocity fluctuations on the Jakobshavn Isbræ, Greenland. Past studies have shown that ice front retreat is the main trigger of large fluctuations in ice velocity, however, the results here show a potential linkage between draining events and the glacier velocity fluctuations. For instance, between 1st July – 25th July, 2019 I found a speed-up of 856 m yr^{-1}, which coincides with a total lake area decrease of 6.4 km^2. I also found, in agreement with other studies, that draining events alone should not account for all velocity variability, with terminus position and mélange rigidity both acting as main drivers.

ACKNOWLEDGEMENTS

I would foremost like to extend my gratitude towards my supervisor Adriano Lemos for suggesting me the project, along with lending me his time and guidance and supplying me with his expertise in the field. I would next like to thank fellow students Jonas Gunnar Darin and Daniel Dehlin for valuable feedback on the writing in the Introduction and Methods. I would finally like to thank my examiner Céline Heuzé and opponent Rebecka Gustafsson for taking the time to read through and give constructive input on the thesis.

TABLE OF CONTENTS

1 INTRODUCTION

In recent decades, glaciers worldwide have been undergoing significant changes (Shepherd et al., 2018). The Greenland Ice Sheet (GrIS), now one of the major sources of global mean sea level rise (van den Broeke et al., 2016), contributed between 1992-2018 an estimated 10.8 ± 0.9 mm to the mean sea level rise due to its ice losses (Shepherd et al., 2020). Some models predict that it will contribute a further 11.2 ± 0.3 mm by 2098 (Machguth et al., 2013). Marine-terminating glaciers gain mass in the accumulation zone primarily by snowfall and lose mass in the ablation zone through three distinct processes: melting, sublimation, and calving (Chu, 2014). The relationship between the accumulation and ablation rates through melting and sublimation is commonly referred to as the glaciers surface mass balance (SMB) (Mouginot et al., 2019). The GrIS SMB has been persistently negative since 1998, along with consecutive years of unprecedented ice loss between 2006-2012 (van den Broeke et al., 2016; Mouginot et al., 2019). Likewise, Mouginot et al. (2019) estimates a net ice loss of 286 ± 20 Gt between 2010-2018, a six-fold increase since the 1980s. Much of the ice mass loss is a consequence of ice dynamics (i.e. calving rate), which has been suggested to represent roughly 66% of the total ice mass loss since 1972 (Mouginot et al., 2019). This illustrates the importance of understanding the underlying aspects controlling ice dynamics of outlet glaciers.

During the summer season positive net energy flux between the atmosphere and the ice sheet surface drives the generation of surface meltwater which can percolate down through the ice or collect in supraglacial streams (Chu, 2014). These accumulate into lakes or slush zones in topographic depressions on the glacier surface, where the water can be drained further into englacial and subglacial conduits through cracks and moulins through hydro-fracture (Zwally et al., 2002; Chu, 2014). It is not uncommon that these lakes empty in a matter of hours (Das et al., 2008; Doyle et al., 2013), also known as rapid draining events, causing large surges of meltwater into the GrIS (Chu, 2014). Multiple studies have found that increased meltwater input cause changes to the ice sheet dynamics, resulting in glacier speed-up, thinning and increased ice discharge (Zwally et al., 2002; Das et al., 2008; Palmer, Shepherd, Nienow, & Joughin, 2011; Doyle et al., 2013). If excessive amounts of meltwater overburdens the existent subglacial channels, positive pressure differences at the ice-bedrock interface cause local glacial uplift and enhanced basal sliding (Bartholomaus, Anderson, & Anderson, 2008; Das et al., 2008; Doyle et al., 2013).

It has also been shown that throughout the course of the summer season, the meltwater effect on ice dynamics decreases as englacial and subglacial drainage systems adapt to greater efficiency (Bartholomaus et al., 2008; Hoffman, Catania, Neumann, Andrews, & Rumrill, 2011). It has previously been hypothesized that there exists a positive feedback loop between increased surface melt and ice

dynamics (Zwally et al., 2002; Parizek & Alley, 2004). However, further research demonstrate that up to a critical rate of water flow, channelization and glacier deceleration take place as opposed to glacier speed-up (Schoof, 2010; Sundal et al., 2011). Magnússon, Björnsson, Rott, and Pálsson (2010) demonstrate that steady meltwater flowrates lead to long-term decreased basal sliding since it reduced subglacial water pressures. This is instigated by frictional heating of the water flow which enlarges the englacial channels to accommodate increased meltwater volumes (Cowton et al., 2013; Chu, 2014). Between 1990-2007 the average annual GrIS velocities decreased by 10% despite an increased amount of meltwater during the same period (van de Wal et al., 2008). Short-term meltwater pulses (e.g. rapid draining events) play a seemingly larger role for increased ice speed velocities than mean annual melt in general (Schoof, 2010).

STUDY AREA

Jakobshavn Isbræ (JI) is located on the west coast of Greenland, covering a wide area of roughly 70 x 50 km (*Figure 1*). JI is a marine-terminating glacier ending in the Ilulissat Icefjord in Disko Bay, and is one of the fastest flowing outlet glaciers of the GrIS (Mouginot et al., 2019), with velocities reaching 10 km yr^{-1} near the ice front (Joughin, Shean, Smith, & Floricioiu, 2020). Since 2012, the ice speeds at JI have been successively decreasing, however the latest 2019 summer season presented higher rates of ice flow compared to the previous two years (Lemos et al., 2018; Joughin et al., 2020).

Ice velocity changes at JI is strongly correlated to the ice front variation, the main trigger to seasonal velocity variability (Lemos et al., 2018; Joughin et al., 2020). Recent evidence also suggests that mélange rigidity, which is a conglomerate of sea ice and icebergs beyond the calving front (Amundson et al., 2010), has a considerable effect on ice speed velocity and ice thickness, which has been influenced by surrounding oceanographic conditions (Joughin et al., 2008; Khazendar et al., 2019; Joughin et al., 2020). In 1997, following an influx of relatively warm water into Disko Bay from the Irminger Sea, the floating ice tongue disintegrated upon which the calving rate increased, the terminus retreated and ice speeds doubled by the year 2000 (Holland, Thomas, Deyoung, Ribergaard, & Lyberth, 2008). A recent study suggested that a partially grounded and partially floating rigid mélange, coinciding with cooler waters in Disko Bay during the 2016-2018 winter seasons, caused buttressing which suppressed calving to such an extent that the glacier terminus advanced nearly 6 km compared to prior years, slowing down and thickening the ice (Khazendar et al., 2019).

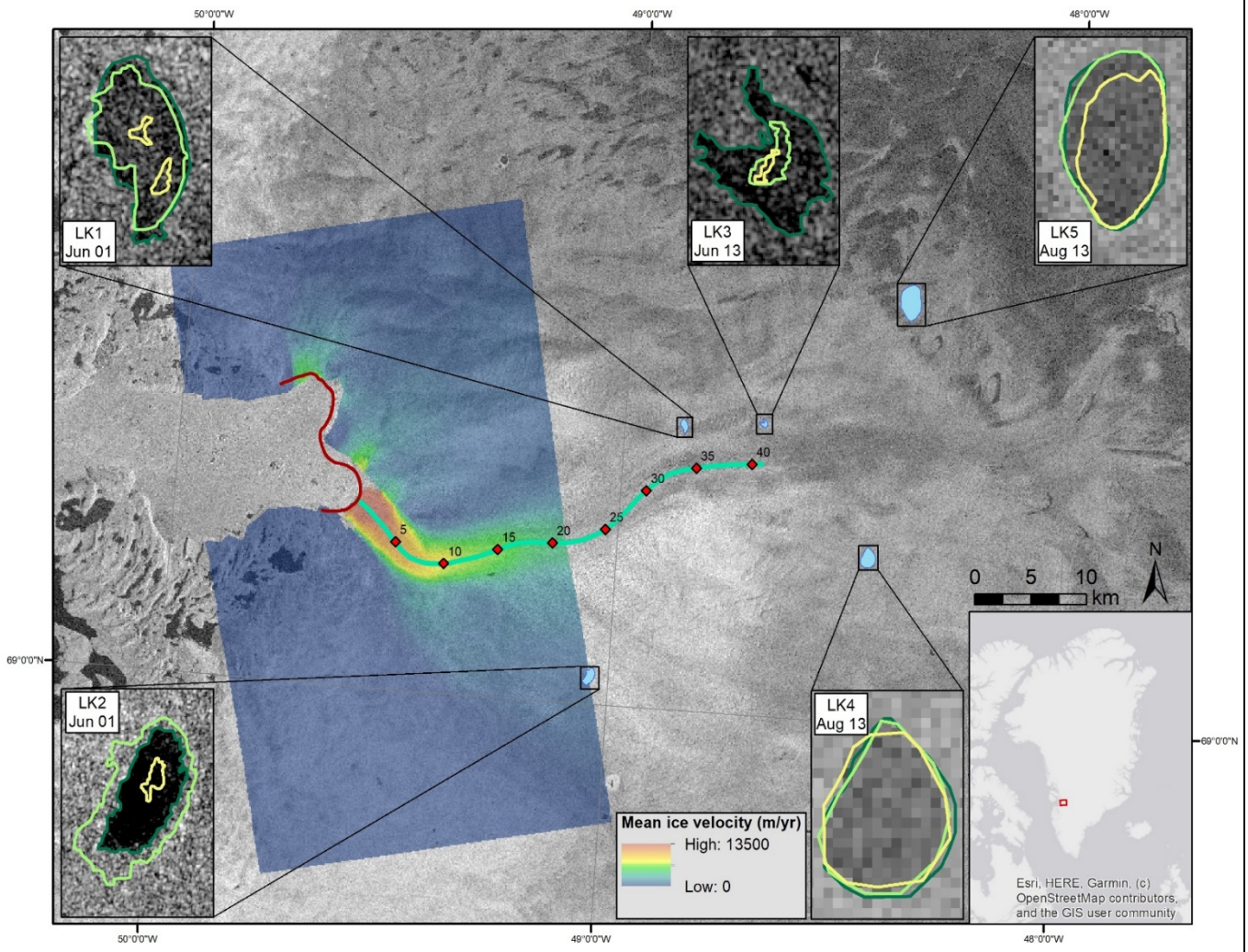

Figure 1: *SAR backscatter intensity overview map of the study region. The red line indicates the glacier calving front and the turquoise line an along-flow transect with 5 km intervals recorded from the calving front. Mean ice velocity over the summer season is also displayed. The locations of the five lakes examined in this study are shown (annotated LK1, LK2 etc.), along with up-close images demonstrating the lakes fluctuations in area coverage (going from dark green → light green → yellow over time, starting from the specified date). The background image was captured 2019-07-20 09:52:10 UTC.*

2 METHOD

2.1 SENTINEL-1 IMAGES

Optical remote sensing data has been used to observe glacier characteristics since the 1970s (Della Ventura, Rampini, Rabagliati, & Barbero, 1983) and collect supraglacial lake information, such as that acquired from the Landsat, MODIS and Sentinel-2 satellite platforms (Box & Ski, 2007; Morriss et al., 2013; Pope et al., 2016). However, optical satellite platforms have limitations due to cloud coverage as well as being daylight dependent (Marshall, Dowdeswell, & Rees, 1994). Synthetic aperture radar

(SAR) Sentinel-1 images, on the other hand, have none of these limitations as it operates with a C-Band active sensor that runs in the microwave frequency (5.404 GHz) which can penetrate through cloud cover (European Space Agency, 2020). Two Sentinel-1 satellites are currently in operation, Sentinel-1A and Sentinel-1B, launched in 2014 and 2016 respectively. The two satellites combined have a revisit time of 6 days over the same orbit but can be higher when taking into consideration orbit overlap at higher latitudes (European Space Agency, 2020). The returned signal to the sensor is known as backscatter, which is a measure of the reflective strength of the ground cover of which the brightness amplitude is registered to construct an image of the scene. Liquid water happens to have a very low reflectance, and as a result will appear as dark spots compared to the surrounding environment (European Space Agency, 2020).

2.2 DATA DOWNLOAD

The Sentinel-1 images were accessed and downloaded through the Copernicus Open Access Hub (https://scihub.copernicus.eu/). I used high resolution Level-1 Ground Range Detected (GRD) SAR images acquired in the Interferometric Wide (IW) swath mode and HH polarization. Each scene covers a 250 km wide area with a 10 x 10-meter pixel size (European Space Agency, 2020). A total of 14 images were acquired between 1st June to 11th September 2019. Time between images varied from 5-12 days where the key point was to capture lake size fluctuations over time. Only images which contained the area of interest in a single scene were used to decrease processing times, and as a result full temporal resolution offered by the Sentinel-1A and 1B satellites were not employed.

2.3 PRE-PROCESSING AND LAKE DETECTION

Each Sentinel scene was pre-processed through the Sentinel-1 toolbox available through the Sentinel Application Platform (SNAP v.7.0.3 – blue boxes in *Figure 2*). The images were first subset to allow for full resolution (10 x 10 m) processing when additional clarity was needed. Then, I followed the following steps (Minchella & Hogg, 2016): (1) Apply Orbit File, which provides an accurate satellite position of the image and velocity information; (2) Thermal Noise Removal, which removes additive noise; (3) Calibration, which converts digital pixel values into a radiometrically calibrated SAR backscatter coefficient (σ^0); and (4) Terrain Correction using the ACE30 DEM, which aims to remove distortion caused by topography and side viewing angles.

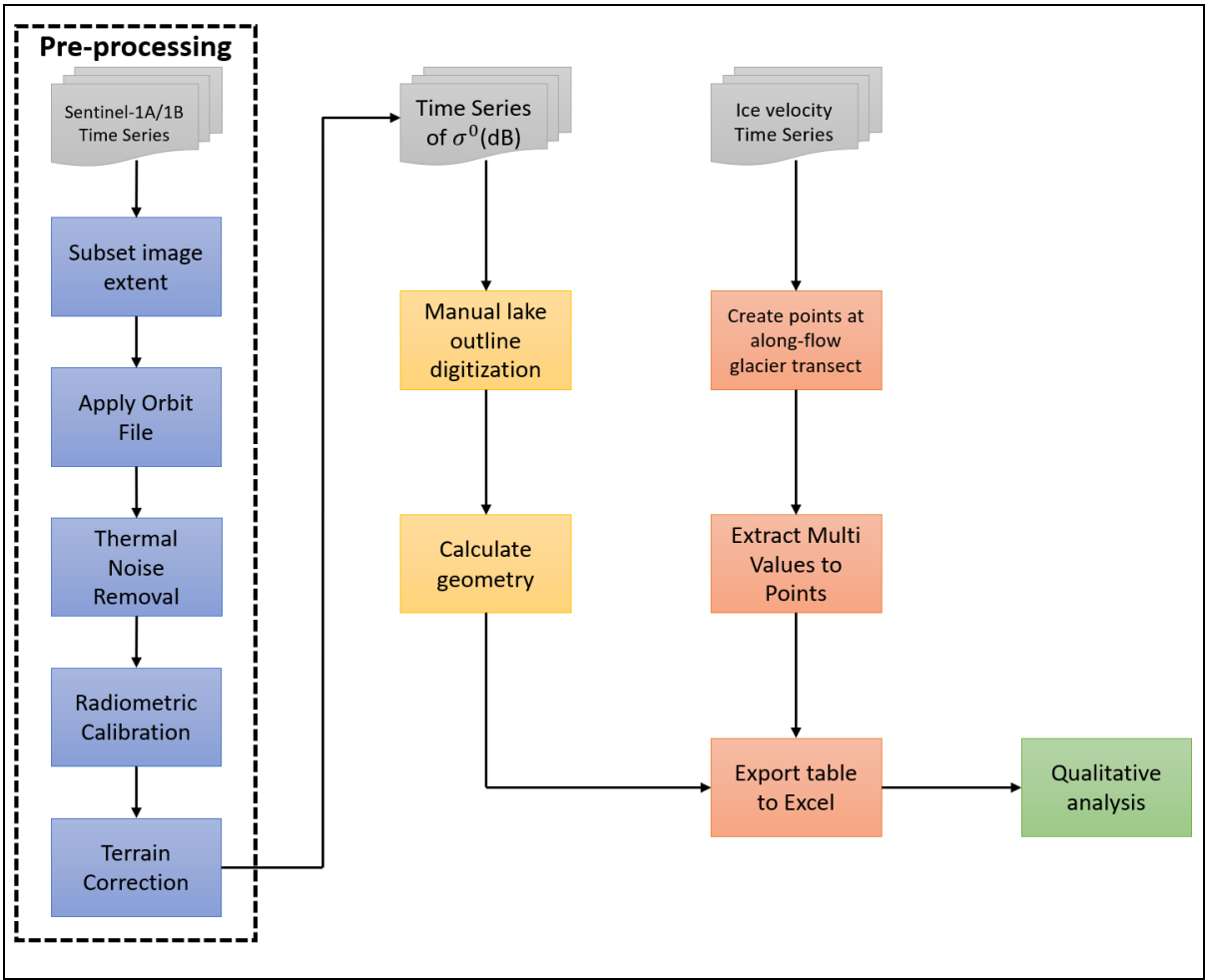

Figure 2*: Flowchart of the complete methodology. Blue boxes indicate processes completed in SNAP, yellow and red boxes in ArcMap and the green box in Excel.*

Lake digitization was done through ArcMap (yellow boxes in *Figure 2*). For visualization purposes, the images were first converted to decibel values using a logarithmic transformation through Raster Calculator: $10 * log10(\sigma^0)$. Due to the speckled backscatter nature of SAR imagery, lake detection and digitization was performed manually as opposed to automatic classification algorithms. I chose a total of five lakes surrounding the main ice stream (*Figure 1*). The lake extents were digitized for each image scene (*Figure 3*), creating a time series of lake area change. I calculated the geometry of the lake area for each date using the *Calculate geometry* tool and exported the time series to Microsoft Excel for further analysis.

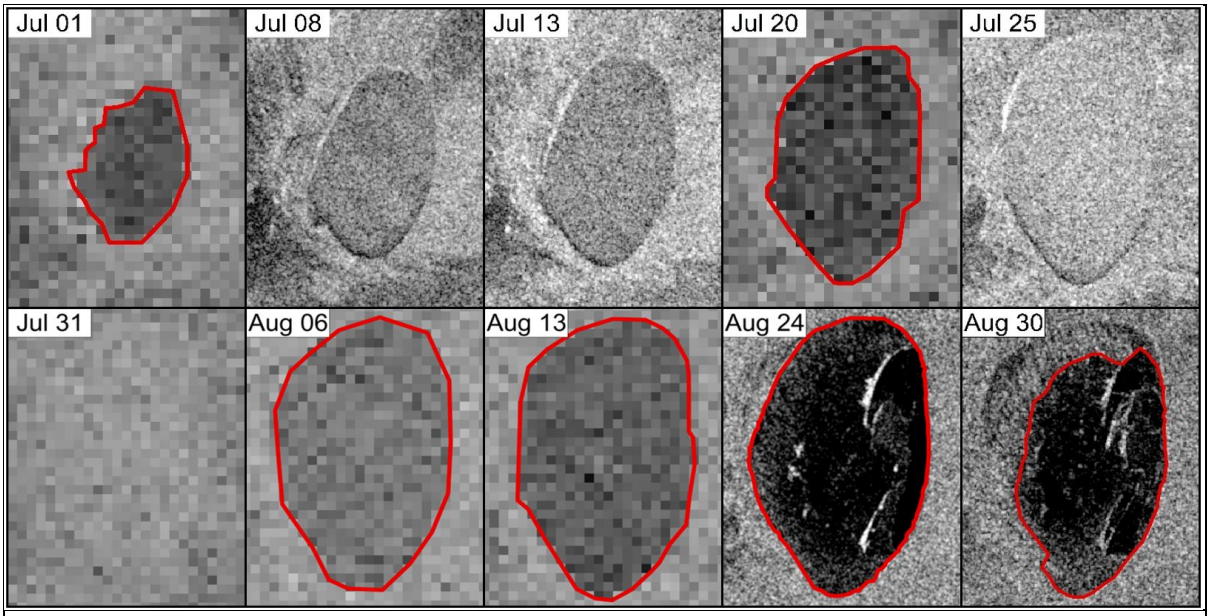

Figure 3: *The variation of LK5 (Figure 1) size under the summer season. On Jul 08, 13, 25 and 31 the lake appeared empty which indicates a draining event took place. For the other dates, the lake extent digitization is shown in red.*

2.4 ICE VELOCITY DATASET

Ice velocity data is produced and made available through the National Snow and Ice Data Center (NSIDC) data portal and is part of a larger NASA project called Making Earth System Data Records for Use in Research Environments (MEaSUREs) (NSIDC, 2020). Each velocity image is produced through interferometric and speckle tracking methods using TerraSAR-X satellite images by tracking the movement of features between two images, and they are posted in 100-meter spatial resolution. (Joughin, Smith, Howat, Scambos, & Moon, 2010; Joughin, Howat, Smith, & Scambos, 2019). What is presented is the mean ice velocity between the two dates of image capture. A total of 10 ice velocity images were analysed, starting 20th May, and ending 18th September 2019. In order to analyse the velocity changes due to the lake drainage variations, I chose three points along the main flow transect (hereafter referred to as points 1, 2 and 3, *Figure 4*). These points are spaced by roughly 8 km between them, and they present high velocity variations (Lemos et al., 2018). The raster pixel values from each of the ice velocity images at points 1, 2 and 3 were recorded using the *Extract multi values to points* tool, which was then exported to Excel for qualitative analysis (red boxes in *Figure 2*).

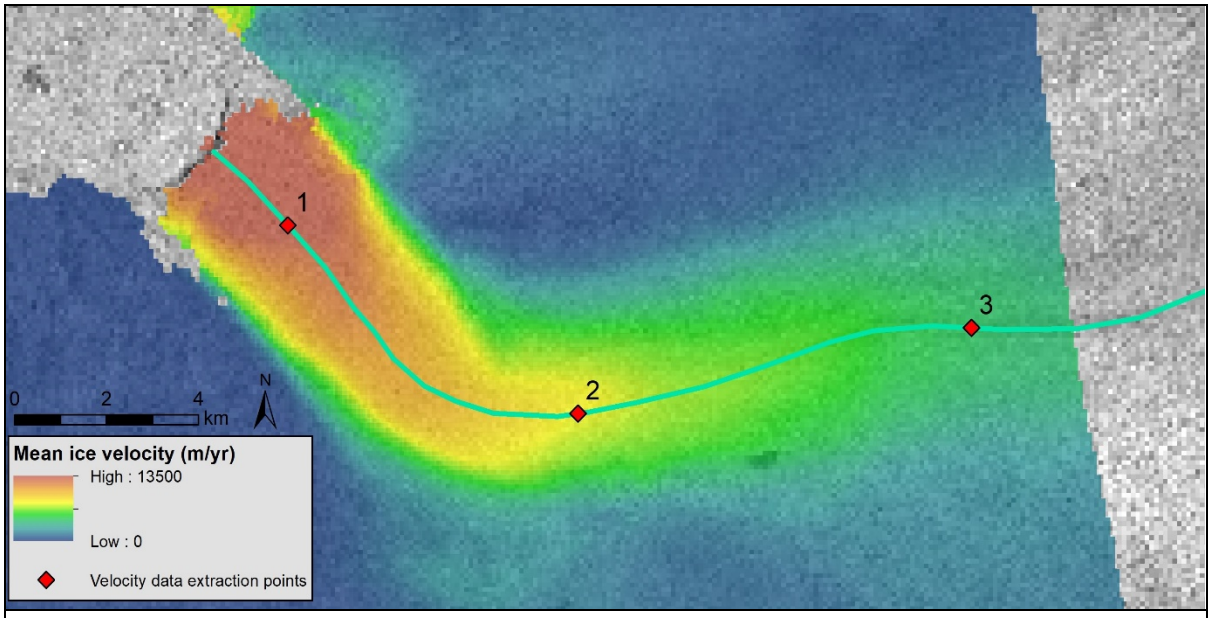

Figure 4: *Overview map presenting the mean ice velocities along the glacier. The red markers indicate the position of ice velocity data extraction points, labeled 1, 2 and 3.*

3 RESULTS AND DISCUSSION

3.1 LAKE AREA CHANGE

Figure 5 and *Figure 6* present high temporal variability in terms of lake formation and drainage, as well as in area changes. The smallest lake, LK3, reached its maximum area extent on 13th June covering roughly 0.3 km^2 while the largest one, LK5, reached its maximum extent on 13th August, covering 4.5 km^2. Krawczynski, Behn, Das, and Joughin (2009) show that lakes which are just 250-800 meters in diameter contain enough water to percolate within a hydro-fracture through a 1 km thick ice-sheet to the base. As the smallest of the lakes analysed in this study, LK3, measures between 550-600 meters across, all lakes should be capable to drain to the base and thus influence the ice velocity. In total, 9 draining events were successfully identified across the five lakes over the entire course of the summer season. The lakes LK1, LK2 and LK3 appeared and subsequently drained during the first third of the season while lakes LK4 and LK5 appeared first in late June and underwent three draining events each. They also accumulated more meltwater than prior each draining event each time.

Figure 3 shows that LK5 appears empty in multiple images, however, this certainly should not mean that there was no surface melt. Most studies argue that once created, a moulin would allow meltwater to continuously flow into the ice sheet throughout the melt season, keeping the moulin open and hindering lake reformation (Das et al., 2008; Doyle et al., 2013; Morriss et al., 2013). In lakes LK4 and LK5 however, the drainage routes became obstructed. This can be observed by not only because they filled up after each draining event, but also due to an increase in area (*Figure 5 and Figure 6*). The

possible cause is a momentary relief of meltwater input, allowing the open moulin to close again via internal ice deformation or ice creep. Catania and Neumann (2010) found that a one meter across, air-filled moulin can close quickly in a matter of days, which would allow meltwater accumulation to restart, filling the depression.

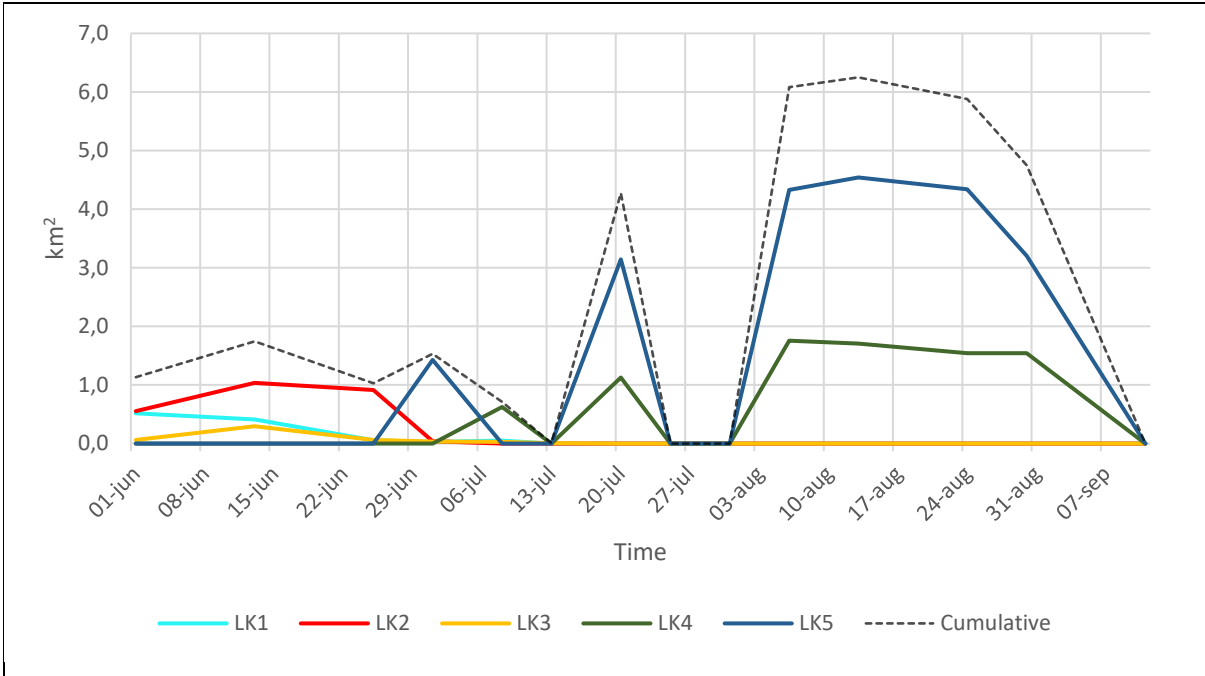

Figure 5: *Total lake area change over time. Graph of total lake area fluctuations over the 2019 summer season in the 5 lakes analysed in this study. Of interest, three draining events take place in LK4 and LK5.*

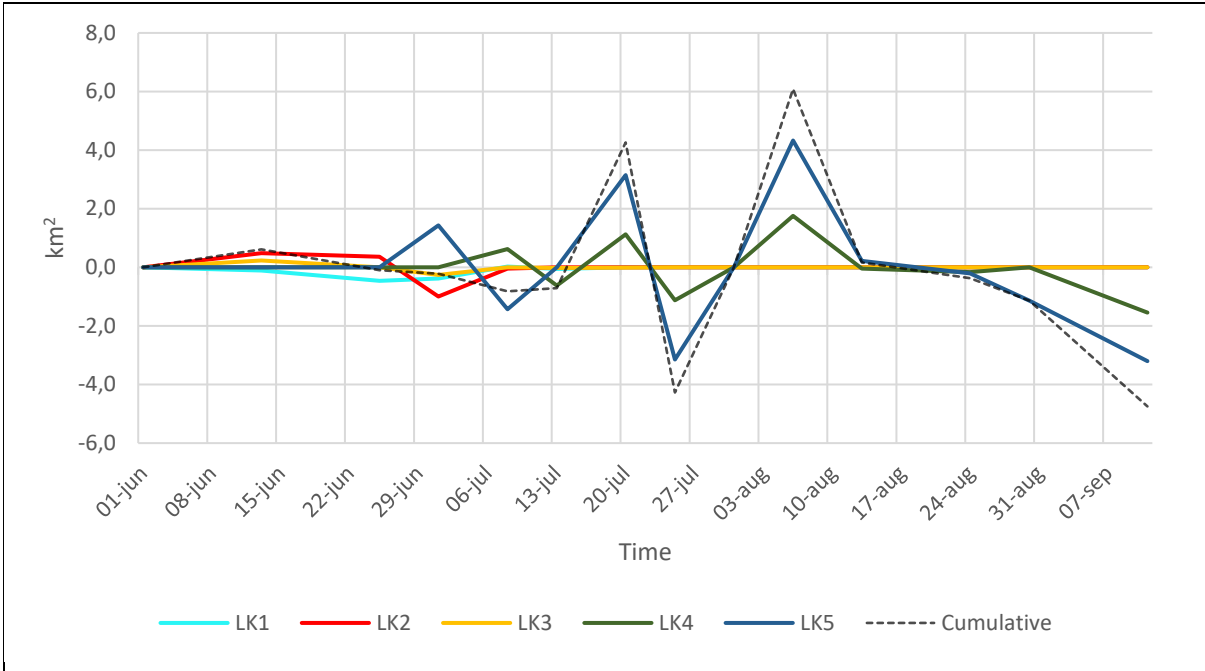

Figure 6: *Graph showing how the lakes have either increased or decreased in size (the change) compared to the previous date. Values above zero indicate meltwater accumulation, at zero indicates no change and below zero indicates that meltwater drainage has occurred.*

3.2 ICE VELOCITY AND LINKS TO DRAINING EVENTS

The ice velocity data in *Figure 7* shows variability throughout the summer season, which evolves progressively from inland towards the ice front where faster ice speeds and velocity variability are found (Lemos et al., 2018). Out of the three points the velocity is at its highest and the most variable at the near-terminus point 1 (*Figure 7*), which will be used as reference in most of the following discussion. Two peaks in ice speed were observed, the first (11400 m yr^{-1}) between 3rd July – 25th July following an increasing trend, before decreasing momentarily to 10600 m yr^{-1}, and then immediately showing another increase until reaching the second peak (11500 m yr^{-1}) between 27th August – 7th September (*Figure 7*).

By visual analyses, the first two draining events of both the larger lakes, LK4 and LK5 (*Figure* 1), take place sometime between 1st July – 25th July, showing a cumulative decrease of 1.8 km^2 and 4.6 km^2 in area respectively (*Figure 5*), which coincides with a velocity increase of 856 m yr^{-1} and an apparent peak in velocity can be seen (*Figure 7*). Additionally, in the following two weeks between 25th July – 5th August, when no rapid draining events were observed (*Figure 5*), I found a velocity decrease of 790 m yr^{-1} (*Figure 7*). Finally, the third and final draining events of lakes LK4 and LK5 take place sometime between 30th August – 11th September and 24th August – 11th September, respectively (*Figure 5*). A decrease of 1.5 km^2 can be observed for LK4 and 4.3 km^2 for LK5. This coincides with a 245 m yr^{-1} velocity increase, which results in the second, larger peak in the late summer between 27th August – 7th September, after which the velocity again decreases (*Figure 7*).

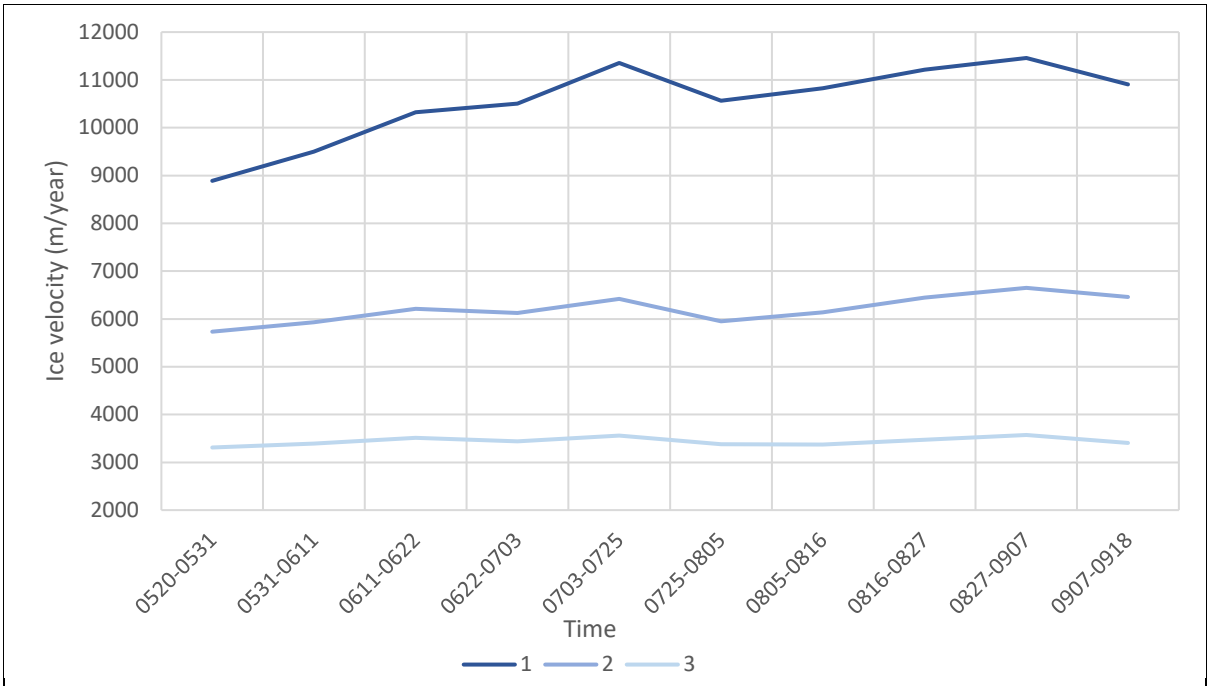

Figure 7: *Ice velocity variability at points 1, 2 and 3 on Jakobshavn Isbræ. Each datapoint represents the mean velocity between the two stated dates.*

The lakes LK1 and LK3 drained 0.4 km^2 and 0.3 km^2 between 13th June – 25th June (*Figure 5*), coinciding with an observed increase of 824 m yr^{-1} in ice velocity between 11th June – 22nd June compared to the previous interval (*Figure 7*). During the draining event of LK2, draining roughly 0.9 km^2 between 25th June - 1st July (*Figure 5*), I instead observe velocity decreases at points 2 and 3 and only a small velocity increase at point 1 (*Figure 7*). As the lake LK2 is relatively far from the main ice flow, and is closer to the terminus than the other lakes (*Figure 1*), the water might have percolated and been routed towards the fjord, and not affect the ice velocity at any of the point locations. As the season progresses, the possibility of observing increased ice velocities influenced by rapid draining events is reduced due to the efficiency adaptations of the subglacial drainage network (Bartholomaus et al., 2008; Hoffman et al., 2011). Inefficient drainage should be seen at the start of the melt season, where the first waves of high meltwater input overwhelm underdeveloped drainage conduits, causing a rapid response in form of glacier uplift and enhanced basal sliding, but can be caused throughout the melt season as long as sufficient amounts of meltwater is supplied (Chu, 2014). Sustained meltwater input enlarges and connects the englacial and subglacial channels until the water volume no longer causes overburdened pressure (Chu, 2014).

It is well known that the ice front variation is the main trigger to the seasonal velocity variations at Jakobshavn Isbræ (Joughin et al., 2008; Lemos et al., 2018; Joughin et al., 2020). Between 2012 – 2017 Lemos et al. (2018) estimate a velocity change of 1600 m yr^{-1} per kilometre of calving front retreat. The JI terminus, during the 2019 summer season, retreats from 1st June – 13th June, before plateauing somewhat until 25th June, after which it continues to retreat until 8th July. After this the terminus re-advances until 31st July. Up until this point, the terminus is observed to retreat during ice speed-up and advance during ice slowdown. However, during the second speed-up between 25th July – 8th August and 27th August – 7th September, the terminus position varies between retreat and advance. Additionally, during the 27th August – 7th September ice velocity peak, where you could expect terminus retreat, the terminus advanced nearly 450 meters (*Figure 8*). Joughin et al. (2020) further argues that terminus position is influenced by mélange rigidity, which causes buttressing of the calving front, leading to reduced calving rates and terminus advance. Existing evidence which Joughin et al. (2020) present indeed show that rigid mélange was present during the late summer of 2019, which would explain the observation in terminus position and velocity variability interplay during this time. As this coincides with previously mentioned draining events of a cumulative 5.8 km^2 in lakes LK4 and LK5 in late August/early September (*Figure 5*), this could also be a possible explanation to the velocity increase despite terminus advance.

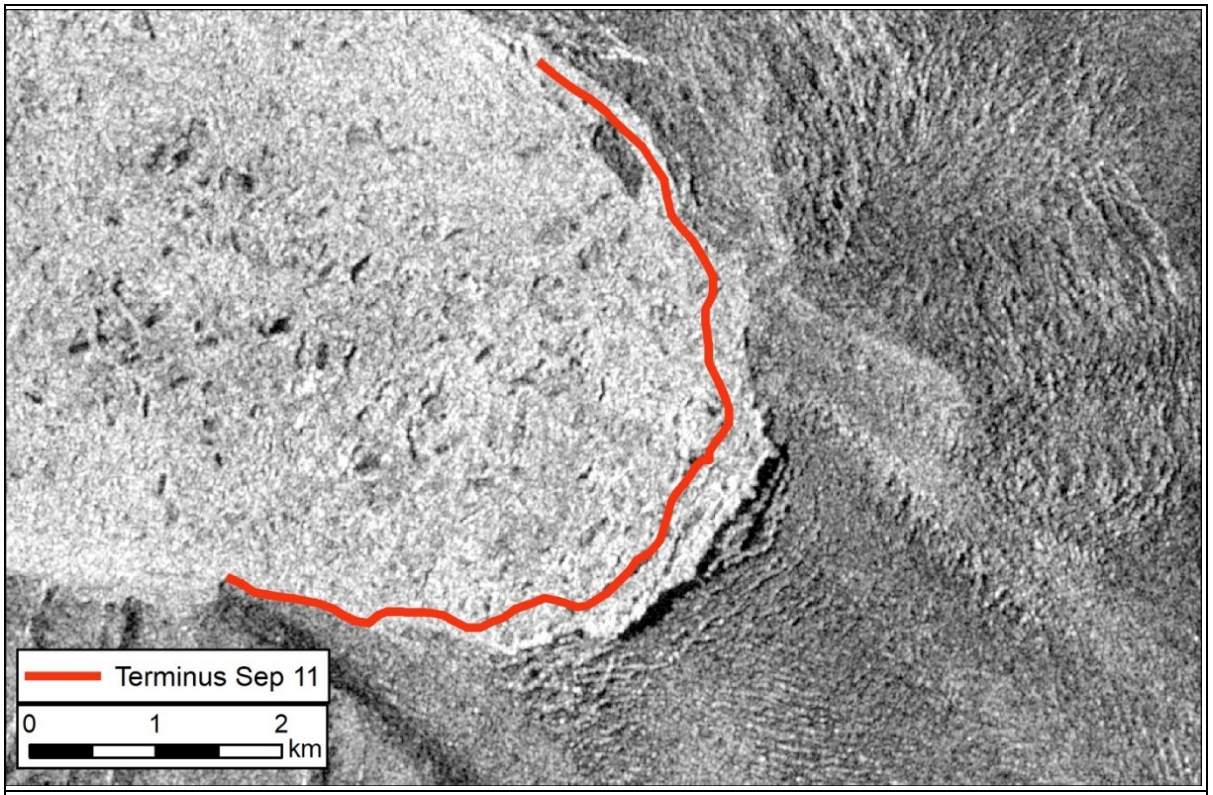

Figure 8: *The terminus advance between 30th August (background image) and 11th September (red line).*

4 CONCLUSIONS AND LIMITATIONS

This study identified multiple supraglacial lake draining events during the 2019 summer season (1st June – 11th September) at the Jakobshavn Isbræ glacier on the west coast of Greenland. I found likely linkages between draining events and ice speed velocity fluctuations. Between 1st July – 25th July I found a speed-up of 856 m yr^{-1}, which coincides with a total lake area decrease of 6.4 km^2 in lakes LK4 and LK5. I also found a velocity increase of 824 m yr^{-1} between 11th June – 22nd June, which coincides with a lake area decrease of 0.7 km^2 in lakes LK1 and LK3. Moreover, until late July the velocity at JI is likely to have been influenced by the terminus position, and in the late summer also have been influenced by a rigid mélange.

Some limitations should well be acknowledged. Through the satellite imagery the time scale over which the draining events take place can be approximately determined, however exact meltwater input volume as well as drainage route remains unknown. This study uses surface lake area coverage as an approximate indicator of the volume of the contained water. All lakes vary in size, shape and form, and so depth, and consequently water volume is not exactly known based on SAR images alone. However, multiple studies have found that area coverage of supraglacial lakes does serve as a reliable

approximation of lake depth and in extension water volume, and has been used extensively in the past (Krawczynski et al., 2009; Liang et al., 2012; Morriss et al., 2013).

Finally, this study makes no attempt in evaluating the timescale over which rapid draining events can affect ice velocity. The temporal resolution of the images observed in this study; mean ice velocity values between every 11-22 days, and 5-12 days of the Sentinel-1 images, are too rough to allow any substantial conclusions about this to be drawn.

5 REFERENCES

Amundson, J. M., Fahnestock, M., Truffer, M., Brown, J., Lüthi, M. P., & Motyka, R. J. (2010). Ice mélange dynamics and implications for terminus stability, Jakobshavn Isbræ, Greenland. *Journal of Geophysical Research: Earth Surface, 115*(F1). doi:10.1029/2009JF001405

Bartholomaus, T. C., Anderson, R. S., & Anderson, S. P. (2008). Response of glacier basal motion to transient water storage. *Nature Geoscience, 1*(1), 33-37. doi:10.1038/ngeo.2007.52

Box, J. E., & Ski, K. (2007). Remote sounding of Greenland supraglacial melt lakes: implications for subglacial hydraulics. *Journal of Glaciology, 53*(181), 257-265. doi:10.3189/172756507782202883

Catania, G. A., & Neumann, T. A. (2010). Persistent englacial drainage features in the Greenland Ice Sheet. *Geophysical Research Letters, 37*(2). doi:10.1029/2009GL041108

Chu, V. (2014). Greenland ice sheet hydrology: A review. *Progress in Physical Geography, 38*, 19-54. doi:10.1177/0309133313507075

Cowton, T., Nienow, P., Sole, A., Wadham, J., Lis, G., Bartholomew, I., . . . Chandler, D. (2013). Evolution of drainage system morphology at a land-terminating Greenlandic outlet glacier. *Journal of Geophysical Research: Earth Surface, 118*(1), 29-41. doi:10.1029/2012JF002540

Das, S. B., Joughin, I., Behn, M. D., Howat, I. M., King, M. A., Lizarralde, D., & Bhatia, M. P. (2008). Fracture propagation to the base of the Greenland Ice Sheet during supraglacial lake drainage. *Science (New York, N.Y.), 320*(5877), 778. doi:10.1126/science.1153360

Della Ventura, A., Rampini, A., Rabagliati, R., & Barbero, R. S. (1983). Glacier monitoring by satellite. *Il Nuovo Cimento C, 6*(2), 211-222. doi:10.1007/BF02507934

Doyle, S. H., Hubbard, A. L., Dow, C. F., Jones, G. A., Fitzpatrick, A., Gusmeroli, A., . . . Box, J. E. (2013). Ice tectonic deformation during the rapid in situ drainage of a supraglacial lake on the Greenland Ice Sheet. *The Cryosphere, 7*(1), 129-140. doi:10.5194/tc-7-129-2013

European Space Agency. (2020). Sentinel-1 SAR User Guide. Retrieved from https://sentinel.esa.int/web/sentinel/user-guides/sentinel-1-sar

Hoffman, M. J., Catania, G. A., Neumann, T. A., Andrews, L. C., & Rumrill, J. A. (2011). Links between acceleration, melting, and supraglacial lake drainage of the western Greenland Ice Sheet. *Journal of Geophysical Research: Earth Surface, 116*(F4). doi:10.1029/2010jf001934

Holland, D., Thomas, R., Deyoung, B., Ribergaard, M., & Lyberth, B. (2008). Acceleration of Jakobshavn Isbr triggered by warm subsurface ocean waters. *Nature Geoscience, 1*, 659-664. doi:10.1038/ngeo316

Joughin, I., Howat, I., Smith, B., & Scambos, T. (2019, 2020). MEaSUREs Greenland Ice Velocity: Selected Glacier Site Velocity Maps from InSAR, Version 2. Retrieved from https://nsidc.org/data/nsidc-0481/versions/2

Joughin, I., Howat, I. M., Fahnestock, M., Smith, B., Krabill, W., Alley, R. B., . . . Truffer, M. (2008). Continued evolution of Jakobshavn Isbrae following its rapid speedup. *Journal of Geophysical Research: Earth Surface, 113*(F4). doi:10.1029/2008JF001023

Joughin, I., Shean, D. E., Smith, B. E., & Floricioiu, D. (2020). A decade of variability on Jakobshavn Isbrae: Ocean temperatures pace speed through influence on melange rigidity. *Cryosphere, 14*(1), 211-227. doi:10.5194/tc-14-211-2020

Joughin, I., Smith, B. E., Howat, I. M., Scambos, T., & Moon, T. (2010). Greenland flow variability from ice-sheet-wide velocity mapping. *Journal of Glaciology, 56*(197), 415-430. doi:10.3189/002214310792447734

Khazendar, A., Fenty, I. G., Carroll, D., Gardner, A., Lee, C. M., Fukumori, I., . . . Willis, J. (2019). Interruption of two decades of Jakobshavn Isbrae acceleration and thinning as regional ocean cools. *Nature Geoscience, 12*(4), 277-283. doi:10.1038/s41561-019-0329-3

Krawczynski, M. J., Behn, M. D., Das, S. B., & Joughin, I. (2009). Constraints on the lake volume required for hydro-fracture through ice sheets. *Geophysical Research Letters, 36*(10). doi:10.1029/2008GL036765

Lemos, A., Shepherd, A., McMillan, M., Hogg, A. E., Hatton, E., & Joughin, I. (2018). Ice velocity of Jakobshavn Isbræ, Petermann Glacier, Nioghalvfjerdsfjorden, and Zachariæ Isstrøm, 2015–2017, from Sentinel 1-a/b SAR imagery. *The Cryosphere, 12*(6), 2087-2097. doi:10.5194/tc-12-2087-2018

Liang, Y.-L., Colgan, W., Lv, Q., Steffen, K., Abdalati, W., Stroeve, J., . . . Bayou, N. (2012). A decadal investigation of supraglacial lakes in West Greenland using a fully automatic detection and tracking algorithm. *Remote Sensing of Environment, 123*, 127-138. doi:https://doi.org/10.1016/j.rse.2012.03.020

Machguth, H., Rastner, P., Bolch, T., Moelg, N., Sorensen, L. S., Agalgeirsdottir, G., . . . Fettweis, X. (2013). The future sea-level rise contribution of Greenland's glaciers and ice caps. *Environmental Research Letters, 8*(2). doi:10.1088/1748-9326/8/2/025005

Magnússon, E., Björnsson, H., Rott, H., & Pálsson, F. (2010). Reduced glacier sliding caused by persistent drainage from a subglacial lake. *The Cryosphere, 4*(1), 13-20. doi:10.5194/tc-4-13-2010

Marshall, G. J., Dowdeswell, J. A., & Rees, W. G. (1994). The spatial and temporal effect of cloud cover on the acquisition of high quality landsat imagery in the European Arctic sector. *Remote Sensing of Environment, 50*(2), 149-160. doi:https://doi.org/10.1016/0034-4257(94)90041-8

Minchella, A., & Hogg, A. (2016). Practicle session: Sentinel-1 ice speed tracking. Retrieved from http://seom.esa.int/cryotraining2016/files/S1_ice_speed_practical_v2.0.pdf

Morriss, B. F., Hawley, R. L., Chipman, J. W., Andrews, L. C., Catania, G. A., Hoffman, M. J., . . . Neumann, T. A. (2013). A ten-year record of supraglacial lake evolution and rapid drainage in West Greenland using an automated processing algorithm for multispectral imagery. *The Cryosphere (Online), 7*(6), 1869-1877. doi:10.5194/tc-7-1869-2013

Mouginot, J., Rignot, E., Bjørk, A. A., van den Broeke, M., Millan, R., Morlighem, M., . . . Wood, M. (2019). Forty-six years of Greenland Ice Sheet mass balance from 1972 to 2018. *Proceedings of the National Academy of Sciences, 116*(19), 9239-9244. doi:10.1073/pnas.1904242116

NSIDC. (2020). MEaSUREs Greenland Ice Velocity: Selected Glacier Site Velocity Maps from InSAR, Version 2. Retrieved from https://nsidc.org/data/nsidc-0481/versions/2

Palmer, S., Shepherd, A., Nienow, P., & Joughin, I. (2011). Seasonal speedup of the Greenland ice sheet linked to routing of surface water. *Earth and Planetary Science Letters, 302*(3-4), 423-428. doi:10.1016/j.epsl.2010.12.037

Parizek, B. R., & Alley, R. B. (2004). Implications of increased Greenland surface melt under global-warming scenarios: ice-sheet simulations. *Quaternary Science Reviews, 23*(9), 1013-1027. doi:https://doi.org/10.1016/j.quascirev.2003.12.024

Pope, A., Scambos, T. A., Moussavi, M., Tedesco, M., Willis, M., Shean, D., & Grigsby, S. (2016). Estimating supraglacial lake depth in West Greenland using Landsat 8 and comparison with other multispectral methods. *The Cryosphere (Online), 10*(1), 15-27. doi:10.5194/tc-10-15-2016

Schoof, C. (2010). Ice-sheet acceleration driven by melt supply variability. *Nature, 468*(7325), 803-806. doi:10.1038/nature09618

Shepherd, A., Ivins, E., Rignot, E., Smith, B., van den Broeke, M., Velicogna, I., . . . The, I. t. (2018). Mass balance of the Antarctic Ice Sheet from 1992 to 2017. *Nature, 558*(7709), 219-222. doi:10.1038/s41586-018-0179-y

Shepherd, A., Ivins, E., Rignot, E., Smith, B., van den Broeke, M., Velicogna, I., . . . The, I. T. (2020). Mass balance of the Greenland Ice Sheet from 1992 to 2018. *Nature, 579*(7798), 233-239. doi:10.1038/s41586-019-1855-2

Sundal, A. V., Shepherd, A., Nienow, P., Hanna, E., Palmer, S., & Huybrechts, P. (2011). Melt-induced speed-up of Greenland ice sheet offset by efficient subglacial drainage. *Nature, 469*(7331), 521-524. doi:10.1038/nature09740

van de Wal, R. S. W., Boot, W., van den Broeke, M. R., Smeets, C. J. P. P., Reijmer, C. H., Donker, J. J. A., & Oerlemans, J. (2008). Large and Rapid Melt-Induced Velocity Changes in the Ablation Zone of the Greenland Ice Sheet. *Science, 321*(5885), 111-113. doi:10.1126/science.1158540

van den Broeke, M. R., Enderlin, E. M., Howat, I. M., Kuipers Munneke, P., Noël, B. P. Y., van de Berg, W. J., . . . Wouters, B. (2016). On the recent contribution of the Greenland ice sheet to sea level change. *The Cryosphere, 10*(5), 1933-1946. doi:10.5194/tc-10-1933-2016

Zwally, H. J., Abdalati, W., Herring, T., Larson, K., Saba, J., & Steffen, K. (2002). Surface Melt-Induced Acceleration of Greenland Ice-Sheet Flow. *Science, 297*(5579), 218-222. doi:10.1126/science.1072708